

## Research Article

# Dynamically Signal Timing Optimization of Isolated Intersection Traffic Lights Based on a Dual-Layer Framework

Junqi Shao , Ke Zhang, Anyou Wang, and Shen Li 

Department of Civil and Engineering, Tsinghua University, Beijing, China

Correspondence should be addressed to Shen Li; [sli299@tsinghua.edu.cn](mailto:sli299@tsinghua.edu.cn)

Received 14 December 2023; Revised 20 March 2024; Accepted 17 May 2024; Published 30 May 2024

Academic Editor: Qixiu Cheng

Copyright © 2024 Junqi Shao et al. This is an open access article distributed under the Creative Commons Attribution License, which permits unrestricted use, distribution, and reproduction in any medium, provided the original work is properly cited.

Intersections are vital components of urban road traffic management, frequently facing persistent congestion challenges. Existing studies rarely combine multiobjective optimization with dynamic adjustment methods. This study introduces an innovative dual-layer framework for traffic signal optimization. The first layer involves multiobjective optimization, addressing critical performance metrics such as delay, the number of stops, and fuel consumption. In the second layer, we propose a method that uses a fuzzy neural network to learn the correspondence between queue lengths and signal timings. This two-tiered approach enables real-time adjustments, achieving dynamic signal optimization. Applying this framework with real traffic flow data to a specific road intersection allows us to determine optimal signal timings dynamically. Extensive simulations using the SUMO software validate the efficacy of our approach in enhancing intersection performance. The timing strategy implemented within this framework leads to a substantial reduction in delay, ranging from 11.1% to 29.0%. The dual-layer framework presented in this study contributes valuable theoretical insights into future research initiatives in this domain.

## 1. Introduction

With rapid economic development, urban traffic control and infrastructure have encountered new demands. As a fundamental driver of economic growth, the transportation industry plays a pivotal role in facilitating the movement of people, goods, and information within a nation's economic activities [1]. Daily urban traffic congestion has become a common concern among the general public. Urban intersections currently need to grapple with heavy traffic flow [2]. Many major cities have attempted measures such as road expansion and the construction of elevated roads to somewhat mitigate congestion [3]. However, these approaches still require further exploration to effectively address the issue of traffic congestion. Addressing traffic congestion necessitates not only measures such as road construction and urban redevelopment but also effective planning and management of motor vehicle traffic [4]. Among the main methods for traffic management, traffic signal control stands out, and many problems stem from inefficient signal timing, particularly in terms of green light

durations for each phase [5]. Significant improvements could be achieved if signal timing could be dynamically adjusted based on traffic flow conditions. In recent years, intelligent connected vehicles and vehicle-to-infrastructure collaboration have rapidly developed. Some traffic flow information can be obtained through these technologies, either from camera-based perception data or vehicle-based perception data, which is more conducive to dynamically adjusting signal timing [6].

Traditional static timing control for traffic signals primarily involves parameters such as cycle length, green ratio, and phase offset. The primary optimization objectives encompass vehicle delay, throughput capacity, and the number of stops [7]. However, many optimization efforts are single-objective. A more advanced approach is multiobjective control, which takes into account multiple optimization objectives and addresses multiobjective problems [8–11].

Using multiobjective optimization for signal timing requires the formulation of a targeted multiobjective optimization model [12, 13]. Generally, fundamental evaluation metrics for measuring traffic flow include delay duration, the

number of stops, capacity, and saturation [14]. Additional metrics may encompass energy consumption, fuel consumption, tire wear, and mechanical wear. Given China's status as a major energy consumer and national goals for energy conservation and carbon neutrality, fuel consumption has become a crucial control metric [15]. Regarding fuel consumption models, literature analysis reveals models established based on total distance, total delay time, and the number of stops [16]. Some scholars determine fuel consumption models based on vehicle speed [17]. Numerous influencing factors can be considered, including emissions and noise as environmental impact indicators, as well as traffic operation costs [18].

Following a research-oriented approach, defining optimization objectives, conducting relevant studies, and establishing multiobjective optimization models are essential. One approach involves transforming the problem into a single-objective one, assigning weights to different influencing factors, and performing a linear combination [19]. However, existing studies often rely on empirical methods for weight assignment, and the incongruent dimensions of various objectives result in inaccuracies. A slight change may lead to a significant variation, indicating poor robustness of the model [20]. Another approach is to directly solve the multiobjective problem, which can avoid the issues mentioned earlier. Simultaneously, it can yield more Pareto solutions, constituting the Pareto optimal solution set [21]. While offering more solutions, this method is relatively computationally intensive and becomes challenging to handle when there are numerous objectives. It also increases the difficulty of selecting an optimal solution from the Pareto solution set [22].

Nevertheless, regardless of the methodology used, these solutions tend to neglect the stochastic nature of traffic flow, rendering them less suitable for abrupt fluctuations in traffic volume. To address this challenge, we choose to adopt a two-layer framework. The first layer utilizes a multiobjective optimization algorithm to obtain a basic solution. Based on this solution, the green light time is dynamically adjusted in the second layer according to the queue length. The method involves generating optimal signal timing for different queue lengths through simulation and then using a fuzzy neural network to learn the corresponding rules from these solutions. This learned rule is then applied to subsequent dynamic green light time adjustments. This approach ensures both basic optimization effectiveness and adaptability to random traffic volume fluctuations.

In this study, the proposed solution combines fundamental evaluation metrics and energy consumption metrics, intending to consider three primary indicators: delay duration, the number of stops, and fuel consumption. The existing literature has relatively few cases that integrate these two factors, and the research in this regard needs to be more comprehensive. The aim is to start from this point and derive new conclusions and discoveries. Furthermore, we apply a fuzzy logic approach based on empirically measured traffic flow data to establish corresponding signal timings for different traffic scenarios. Simulation software is used to

gather real-time data at intersections using sensors and implement the corresponding signal timing adjustments, thereby achieving dynamic timing adaptations. The contributions can be summarized as follows:

- (1) A novel dual-layer framework is proposed, with the first layer conducting multiobjective optimization to obtain a base solution and the second layer performing dynamic adjustments based on this solution. It calculates different green light times corresponding to varying queue lengths, enabling dynamic signal optimization.
- (2) In the second layer, optimal correspondences between queue lengths and signal timings based on real measurement data were generated through simulation. The study utilized a fuzzy neural network to learn the corresponding rules.
- (3) This research uses a new hybrid multiobjective particle swarm algorithm to achieve signal timing optimization. Fuel consumption is introduced as a key factor in the multiobjective optimization model, showcasing its potential as a robust tool for signal timing optimization.

The rest of this paper is organized as follows: In the Methods section, we introduce the objective function and elucidate the principles of the algorithms. In the Experimental Design section, real-world data collection is discussed, outlining the research approaches and steps for each layer of the two-layer framework. In the Results and Analysis section, the process of obtaining dynamic signal timing through the two-layer framework, the simulation implementation of dynamic signal timing, and the analysis of the resulting data are presented.

## 2. Methods

This section provides an in-depth exploration of methodologies used to determine target values for individual optimization objectives in a multiobjective model, along with the calculation methods for specific parameters within the model's formulas. Furthermore, it introduces the principles behind the multiobjective optimization algorithm used.

In addressing the multiobjective problem, the MOPSO algorithm and the NSGAI-MOPSO algorithm are used. The green signal time corresponding to queue length is determined and applied using a fuzzy neural network approach. The schematic structure of the dual-layer framework is shown in Figure 1.

*2.1. Multiobjective Problem Definition.* Currently, there is relatively limited consideration for combining delay indicators with energy-related indicators such as fuel consumption. In this study, delay, number of stops, and fuel consumption are comprehensively considered as the objective functions to establish a dynamic signal control optimization model for intersections.

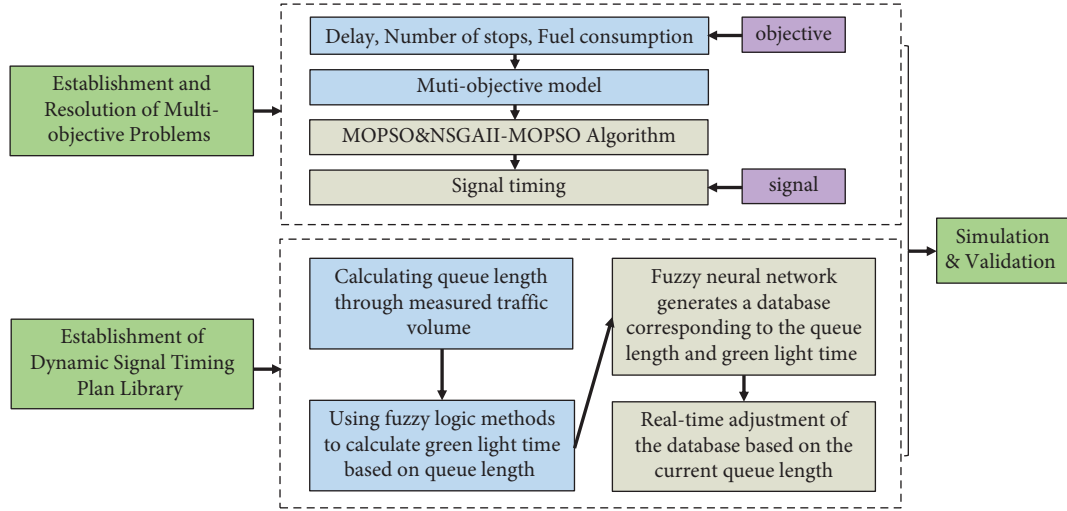


FIGURE 1: The dual-layer framework structure for the dynamic signal timing problem.

**2.1.1. Delays.** Delay is primarily caused by traffic resistance and traffic control, resulting in travel time losses. It is closely related to indicators such as cycle length, green signal ratio, and saturation. This paper introduces an improved delay time calculation model and the concept of critical traffic flow. The term critical traffic flow refers to the flow of traffic from an inlet lane that has the highest flow rate ratio in each signal phase. It can be considered a representative of all traffic flows in that phase and is referred to as the critical traffic flow. Therefore, formula (1) can be used to better describe the delay time model.

$$d_i = \frac{(x_i^{\max})^2}{2 \times q_i^{\max} \times (1 - x_i^{\max})} + \frac{C \times (1 - g_i/C)^2}{2 \times (1 - y_i^{\max})}. \quad (1)$$

In the equations,  $i$  is the  $i$ -th signal phase;  $d_i$  is average delay time for all vehicles in phase  $i$ ;  $g_i$  is green light time for phase  $i$ ;  $C$  is duration of the signal cycle;  $y_i^{\max}$  is the maximum value of the flow ratio for phase  $i$  among all entry lanes;  $y_{ij}$  is the flow ratio for the  $j$ -th entry lane of phase  $i$ ;  $x_i^{\max}$  is the maximum value of the saturation degree for phase  $i$  among all entry lanes;  $x_{ij}$  is the saturation degree for the  $j$ -th entry lane of phase  $i$ ;  $q_i^{\max}$  is the maximum value of traffic volume for phase  $i$  among all entry lanes;  $q_{ij}$  is equivalent traffic volume for the  $j$ -th entry lane of phase  $i$ ; and  $q_i$  is equivalent traffic volume for phase  $i$ .

**2.1.2. Number of Stops.** Due to the influence of traffic signals, upstream traffic often arrives in the form of platoons. To ensure the continuous passage of these platoons through the intersection without interruptions and prevent a significant number of vehicles within the platoons from getting stuck in the lanes, which could result in reduced intersection capacity, controlling the number of stops is also crucial. The improved method for calculating the stopping rate similarly introduces the concept of “critical traffic flow.” This concept is based on analyzing the impact of different inlet-lane traffic flows on the stopping rate within the same phase. The following formula (2)–(4) represents the specific improved calculation formula:

$$h_i = f \left( \frac{1 - g_i/C}{1 - y_i^{\max}} + \frac{N_i}{q_i^{\max} C} \right), \quad (2)$$

$$N_i = \frac{e^k}{2(1 - x_i^{\max})}, \quad (3)$$

$$k = -1.33 \times \sqrt{\frac{m_i^{\max} q_i (1 - x_i^{\max})}{x_i^{\max}}}. \quad (4)$$

In addition to the symbols mentioned earlier, there are the following:  $h_i$  is the number of stops;  $N_i$  is the average excess queue length for phase  $i$ ;  $m_i^{\max}$  is the maximum value of the saturation flow rate for phase  $i$  among all entry lanes; and  $m_{ij}$  is the saturation flow rate for the  $j$ -th entry lane of phase  $i$ .

**2.1.3. Fuel Consumption.** Under different road conditions, loads, and traffic situations, a vehicle’s operational state can vary. On urban roads, due to a variety of traffic factors, vehicle acceleration, deceleration, and unstable driving result in a significant increase in fuel consumption. This interference is primarily associated with delay time and the number of stops, both of which hinge on the signal timing of intersections.

Formula (5) is a fuel consumption model obtained through a linear combination of delay time, the number of stops, and total vehicle travel distance, expressed in terms of fuel consumption.

$$E = f_1 L_s + f_2 d + f_3 h. \quad (5)$$

In the equations,  $L_s$  is total travel distance, calculated as the product of travel mileage and traffic flow rate;  $d$  is total delay time of all vehicles;  $h$  is the sum of the total number of complete stops per hour for all vehicles; and  $f_1$ ,  $f_2$ , and  $f_3$  varies according to different vehicle models.

**2.1.4. Objective Function.** By taking weighted averages based on traffic flow for each phase, the total delay and total stopping rate are calculated. The total delay at the

intersection, the total stopping rate, and the total fuel consumption are then utilized as optimization metrics to establish a multiobjective model, as depicted in the following formula:

$$\begin{cases} \min d = \frac{\sum_{i=1}^n d_i Q_i}{\sum_{i=1}^n Q_i} \\ \min h = \frac{\sum_{i=1}^n h_i Q_i}{\sum_{i=1}^n Q_i} \\ \min E = f_1 L_s + f_2 d + f_3 h. \end{cases} \quad (6)$$

Subsequently, a multiobjective optimization algorithm is used for computation to obtain the optimal solution. Based on this optimal solution, signal timing is dynamically adjusted according to traffic flow. In addition, in this model, constraint conditions consider indicators such as cycle duration, green light duration, and saturation within certain ranges.

## 2.2. The Proposed Dual-Layer Framework Structure

### 2.2.1. First Layer: Multiobjective Optimization Method for Signal Timing.

Particle swarm optimization (PSO) starts with initializing a group of random particles (random solutions). It then iteratively seeks the optimal solution. In each iteration, particles update themselves by tracking two “extremal values” (pbest and gbest). After identifying these two optimal values, particles update their velocities and positions using the following formula:

$$x_i(t) = x_i(t-1) + v_i(t), \quad (7)$$

$$v_i(t) = w \times v_i(t-1) + C_1 \times r_1 \times (x_{pbest_i} - x_i) + C_2 \times r_2 \times (x_{gbest_i} - x_i). \quad (8)$$

Multiobjective particle swarm optimization (MOPSO) is an extension of methods originally designed for single-objective problems to encompass multiple objectives. The elitist nondominated sorting genetic algorithm (NSGAII) is a classic multiobjective genetic algorithm that introduces a fast nondominated sorting algorithm, reducing the computational complexity of nondominated sequence calculations. It incorporates an elitist strategy, broadening the sampling space and enhancing the accuracy of optimization results.

Some scholars creatively integrated two algorithms [23]. In each iteration, the two algorithms are alternated to maintain diversity and nondominated solutions. This hybrid approach helps to better solve multiobjective optimization problems. Table 1 is the pseudocode for the algorithm.

### 2.2.2. Second Layer: Dynamic Adjustment Algorithm for Signal Timing.

The first step in the second layer is the simulation to generate the relationship between queue length and optimal signal extension time.

TABLE 1: Pseudocode for the NSGAII-MOPSO algorithm.

Algorithm
Algorithm: hybrid multiobjective optimization (NSGA-II and MOPSO)
(1) Initialize parameters and populations: Set common, NSGA-II, and MOPSO specific parameters Initialize NSGA-II population “pop_nsga” Initialize MOPSO population “pop_mopso”
(2) For each iteration:
(a) NSGA-II operations: Evaluate and sort “pop_nsga” using nondominated sorting Apply crossover and mutation to generate offspring Merge and truncate “pop_nsga” to maintain population size
(b) MOPSO operations: Update “pop_mopso” positions and velocities Apply mutation operation Store updated positions in “pop_mopso1”
(c) Combine and evaluate: Merge “pop_mopso1” and “pop_nsga” into “pop_combined” Sort “pop_combined” using nondominated sorting Truncate “pop_combined” to maintain size
(3) Output final solution set: Extract and plot the nondominated solutions from “pop_combined” End algorithm

“Simulation of Urban MObility” (SUMO) is an open-source, highly portable, microscopic, and continuous traffic simulation package designed to handle large networks [24]. In the SUMO software, we can configure intersection forms, define traffic flow, and utilize Python with the traffic control interface (TraCI) to achieve real-time traffic information retrieval.

In SUMO simulation, a day of traffic data is generated based on measured traffic flow. The queue lengths are recorded for four phases during this simulation. Using the fixed timing obtained in the first layer, it is iterated around this timing to find the timing that minimizes delay at the intersection. This process establishes a relationship between queue lengths and green light extension time.

The vehicle queue lengths are simulated at different times throughout the day: Based on the previously measured traffic flow at different time intervals, the vehicle queue lengths are simulated for each hour of the 24-hour period.

The second step in the second layer is for the fuzzy neural network to learn the rules for the correspondence between queue length and signal extension time from the generated data.

The adaptive neuro-fuzzy inference system (ANFIS) is a type of fuzzy controller based on the Takagi–Sugeno model. By utilizing neural networks, the ANFIS is capable of automatically recognizing and processing fuzzy information, effectively addressing complex problems through the adaptability of the fuzzy controller. It involves offline training, online learning, and the automatic adjustment of fuzzy inference control rules, enabling it to become adaptive and self-learning.

Under a simple assumption, consider a fuzzy inference system with two inputs,  $x$  and  $y$ , and a single output,  $z$ . This system comprises two fuzzy rules:

Rule 1: if  $x$  is  $A_1$  and  $y$  is  $B_1$  then  $f_1 = p_1x + q_1y + r_1$ .

Rule 2: if  $x$  is  $A_2$  and  $y$  is  $B_2$  then  $f_2 = p_2x + q_2y + r_2$ .

The first-order fuzzy inference system ANFIS network has a structure as shown in Figure 2.

The ANFIS controller, through the application of Sugeno-type fuzzy rules and weighted summation, significantly reduces the complexity of data processing and is more accurate than traditional centroid methods, thereby enhancing system performance. In this paper, the ANFIS model from the MATLAB fuzzy logic toolbox is utilized.

### 3. Experimental Design

The following pertains to data acquisition and signal timing calculation for an actual intersection implemented in simulation software for dynamic signal timing.

**3.1. Data Collection.** To ensure the accuracy of dynamic signal timing simulation, comprehensive data collection is paramount. This process involves the gathering of essential information related to traffic conditions and existing signal timing parameters at the intersection.

**3.1.1. Traffic Volume.** The intersection of Chengfu Road and East Zhongguancun Street in Haidian District, Beijing, was chosen as the experimental intersection. This intersection experiences high traffic and pedestrian flow, as it is formed by the intersection of two arterial main roads. As shown in Figure 3, the four road sections, namely north, west, south, and east, are designated as Sections 1, 2, 3, and 4, respectively.

The traffic flow data for each 10-minute interval of the day at the intersection were measured using counters and recorded in Figure 4.

The daily average flow was obtained by calculating the weighted average for each representative time period. The average hourly flow for each inbound road segment is shown in Tables 2 and 3.

The average hourly flow for each outbound road segment is shown in Table 3.

**3.1.2. Signal Phase.** The intersection has four signal phases, namely, south-north through, south-north left turn, east-west through, and east-west left turn, as illustrated in Figure 5.

The current signal timing for each phase is shown in Figure 6.

**3.2. The Multiobjective Optimization of Signal Timing Based on the First Layer.** Two algorithms, the traditional multi-objective particle swarm algorithm (MOPSO) and a hybrid particle swarm algorithm mixed with a genetic algorithm (NSGAI-MOPSO), are used to solve multiobjective problems. The Pareto fronts of the two algorithms are compared; an optimal solution is selected from the solution set as the result of the first layer in multiobjective optimization; and the robustness of the solution set is analyzed. The logical progression of this part of the work is illustrated in Figure 7.

**3.3. Signal Timing Adjustment Based on the Second Layer.** In the second part of the dual-layer framework, we use a fuzzy neural network to learn the correlation between queue lengths and phase durations. With this information, we construct a database. The logical progression of this part of the work is illustrated in Figure 8.

**3.3.1. Correspondence between Queue Lengths and Signal Timing Obtained from Simulation Data.** In the first part of the second layer, based on the measured data, we simulate traffic flow. At different times, the four road segments have different queue lengths. We iterate through signal timing at the intersection for that specific time, and based on minimizing delay, we determine the optimal signal timing corresponding to the queue length at that moment.

**3.3.2. Fuzzy Neural Network.** In the second part of the second layer, utilizing a fuzzy neural network, we learn corresponding rules from a large dataset of queue lengths and signal timings obtained through simulation based on measured data. With this learned set of rules, real-time dynamic signal timing can be achieved by obtaining queue lengths according to the established rules.

## 4. Results and Analysis

The following timing results are analyzed from the perspective of the two-layer framework. Additionally, the simulation implementation and data analysis of dynamic timing are introduced.

**4.1. The Multiobjective Optimization of Signal Timing Based on the First Layer.** The following utilizes two algorithms to calculate signal timing, compares the Pareto solution sets produced by both algorithms, and then selects an optimal solution as the timing result.

**4.1.1. MOPSO Algorithm and NSGAI-MOPSO Algorithm.** First, the conventional multiobjective particle swarm optimization (MOPSO) algorithm is applied to the timing model along with its constraints. The calculated parameters obtained earlier are incorporated into the constraints. The algorithm is then used to solve the model under these constraints. The iteration count is set to 100, and the initial population is 150. Then, the NSGA-II and MOPSO hybrid algorithms are adopted, with 100 iterations and an initial population of 150. The Pareto solution set is illustrated in Figure 9. Blue represents the MOPSO algorithm, while magenta represents the NSGAI-MOPSO algorithm.

From the solution set, it can be observed that the solutions obtained by the NSGAI-MOPSO algorithm are more densely distributed. Also, it can be observed that the NSGAI-MOPSO algorithm performs better than the MOPSO algorithm in terms of the parking rate, delay time, and fuel consumption.

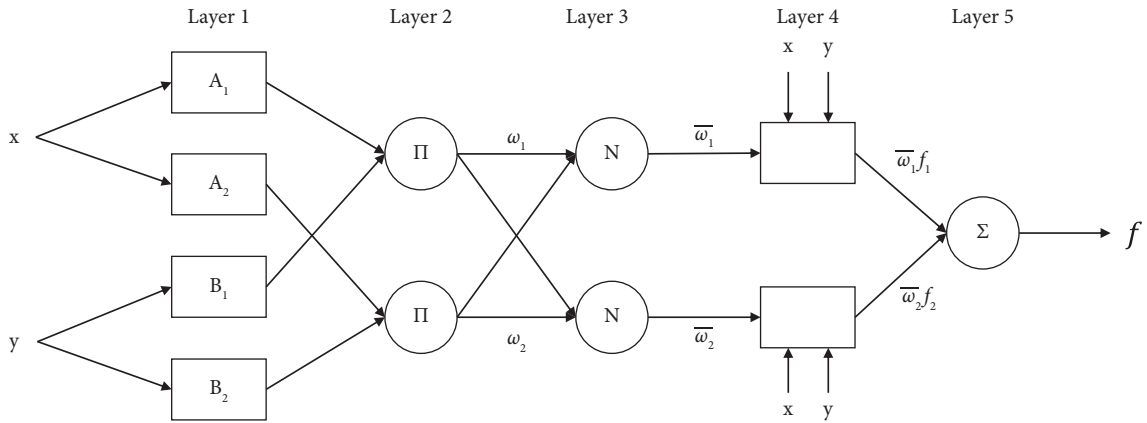


FIGURE 2: ANFIS network structure.

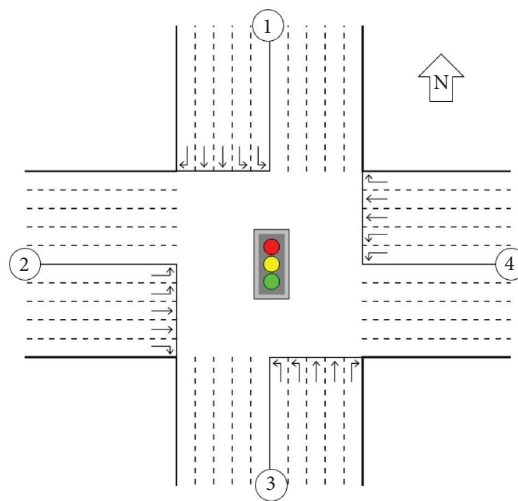


FIGURE 3: Intersection channelization diagram.

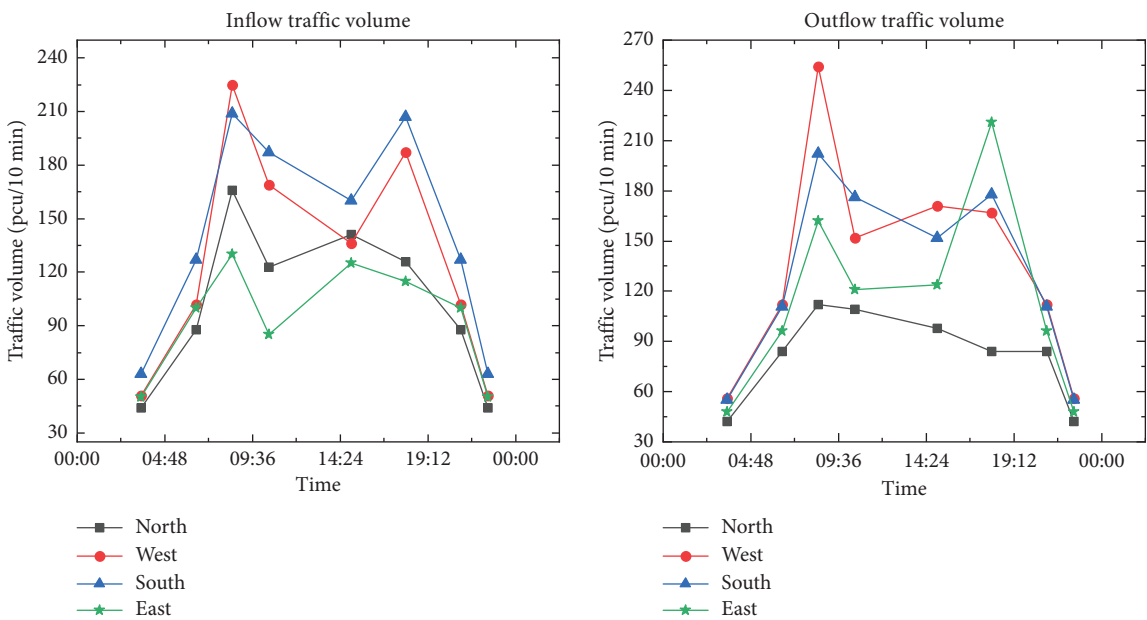


FIGURE 4: Inflow and outflow traffic volume.

TABLE 2: Inflow traffic volume.

Entrance section	I1	I2	I3	I4
Volume (pcu/h)	551	674	758	492

TABLE 3: Outflow traffic volume.

Exit section	O1	O2	O3	O4
Volume (pcu/h)	448	722	705	600

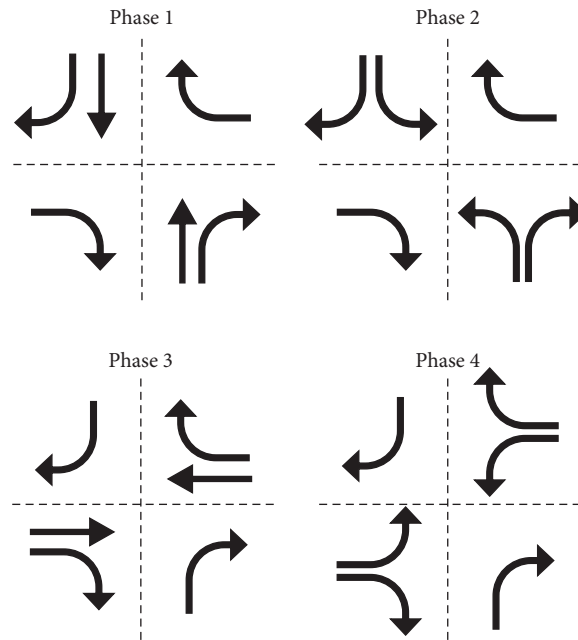


FIGURE 5: Intersection phase diagram.

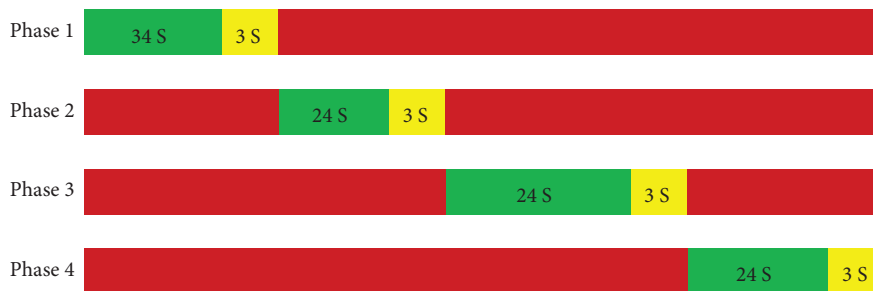


FIGURE 6: Intersection signal timing.

4.1.2. *Selecting an Optimal Solution from the Pareto Solution Set.* From the NSGAI-MOPSO solution set curve, the group of solutions with the slowest growth rate of the parking rate is selected, indicated by the smallest slope of the curve. This solution, with a corresponding delay time of 27.3953 seconds and a parking rate of 0.7597, corresponds to the timing scheme with a cycle length of  $C = 84 + 12$  s and individual phase green times  $g_1 = 26$  s,  $g_2 = 15$  s,  $g_3 = 28$  s, and  $g_4 = 15$  s.

4.1.3. *Robustness Analysis.* Performing a small perturbation on the input data, specifically increasing each input value by 10%, and rerunning the multiobjective optimization program, we observe changes in the Pareto solution set. It can be seen that all three objective values change by less than 10%, indicating that the solution set essentially retains its original form. The optimal solution, selected based on the predefined rules, experiences some changes, but the variation remains

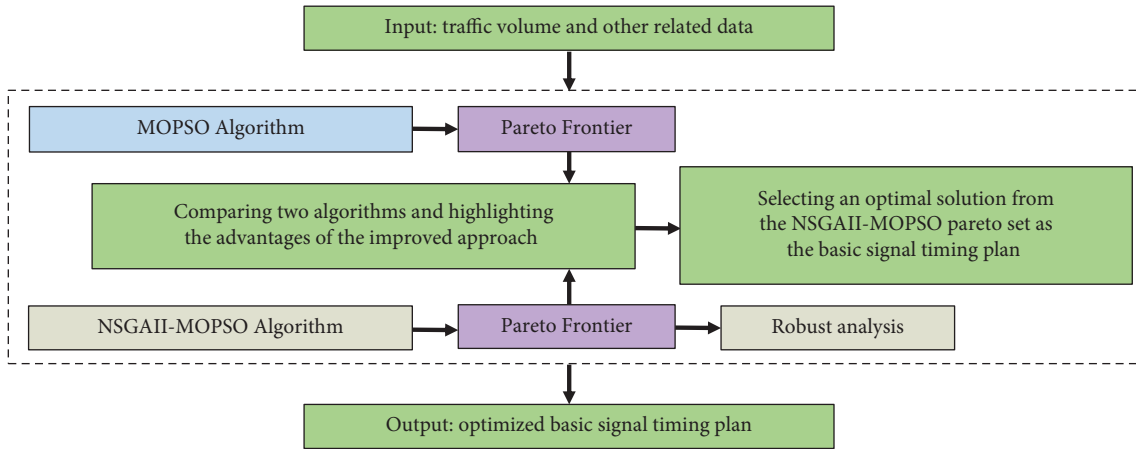


FIGURE 7: The experimental design structure of the first layer.

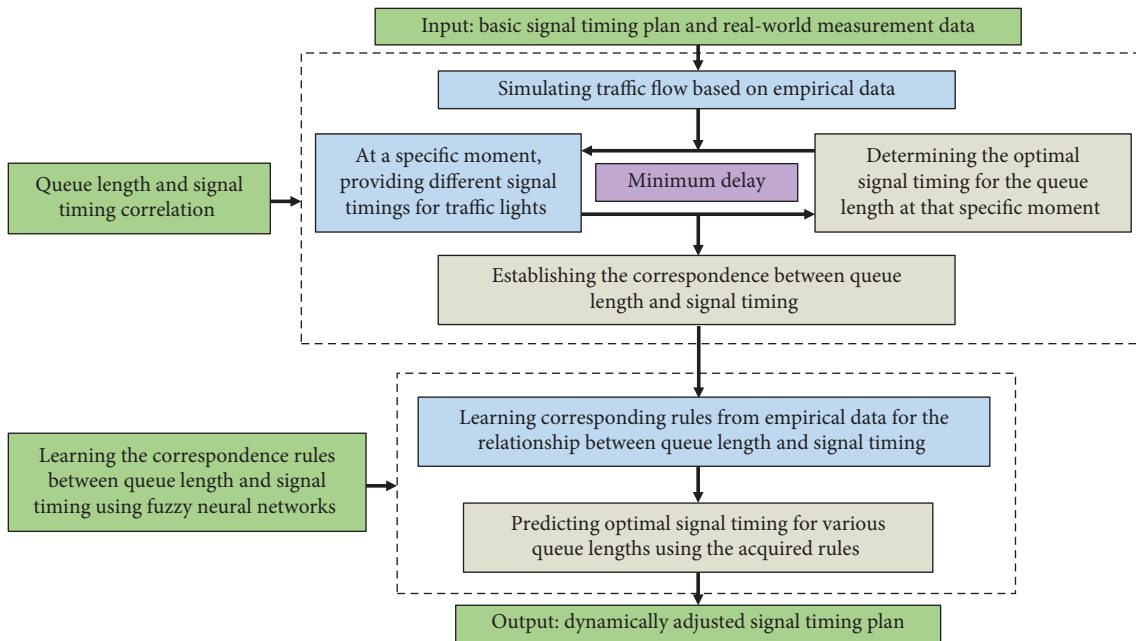


FIGURE 8: The experimental design structure of the second layer.

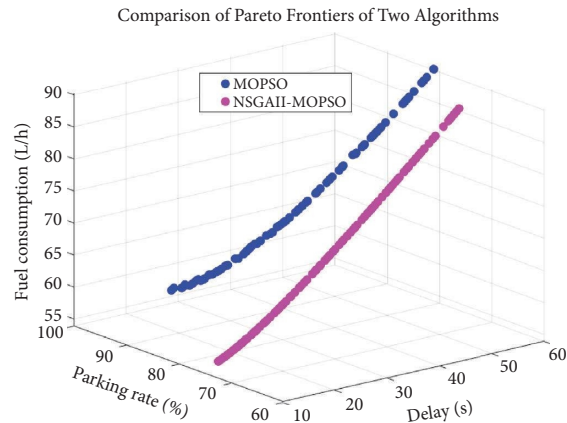


FIGURE 9: Pareto Frontier of the NSGAI-MOPSO algorithm.



within a 10% range. This demonstrates that the algorithm possesses sufficient robustness, showing resilience to small perturbations in the input data.

#### 4.2. Signal Timing Adjustment Based on the Second Layer.

In the second part of the dual-layer framework, we use a fuzzy neural network to learn the correlation between queue lengths and phase durations. With this information, we construct a database.

**4.2.1. Correspondence between Queue Lengths and Signal Timing Obtained from Simulation Data.** The previously measured data are utilized to obtain a significant amount of corresponding data between queue lengths and green light extension times.

The obtained green light extension times at different time intervals are shown in the following Figure 10.

**4.2.2. Fuzzy Neural Network.** Using queue length as fuzzy inputs and the green light extension time obtained from the previous fuzzy logic method as output, a neural network is constructed to predict a large number of specific green light times corresponding to different queue lengths with a unit of 0.5 meters.

This process is implemented using the ANFIS fuzzy neural control toolbox in MATLAB.

An Excel spreadsheet is created, and the fuzzy logic-derived data are utilized as the training set. The current phase queue length and the subsequent phase queue length are used as inputs, with the green light time as the output, to generate a comprehensive database predicting green light times for a diverse range of queue lengths, each with a unit increment of 0.5 meters. This database will be instrumental for dynamic timing applications. Subsequently, the data obtained from the prior fuzzy logic calculations are partitioned into distinct training, validation, and test sets. The fuzzy inference system (FIS) is trained, specifying error thresholds and epochs, and the network model is executed. Figure 11 shows the membership functions of the obtained relationship between queue length and green light extension time through training.

The trained network is used to predict green light times corresponding to queue lengths ranging from 0 to 140 meters with a unit of 0.5 meters. The results are exported to an Excel spreadsheet to serve as a database. According to the obtained green light extension time, added to the basic timing scheme obtained in the previous stage, Figure 12 shows the corresponding relationship between different queue lengths and green light times. It can be observed that, for commonly encountered queue lengths at actual intersections, the optimal green light duration is also a typical range of 18–25 seconds. As the queue length increases, the optimal green light duration rapidly grows.

**4.3. Simulation Validation.** This section utilizes the SUMO simulation software for data simulation verification and implements signal timing within the software.

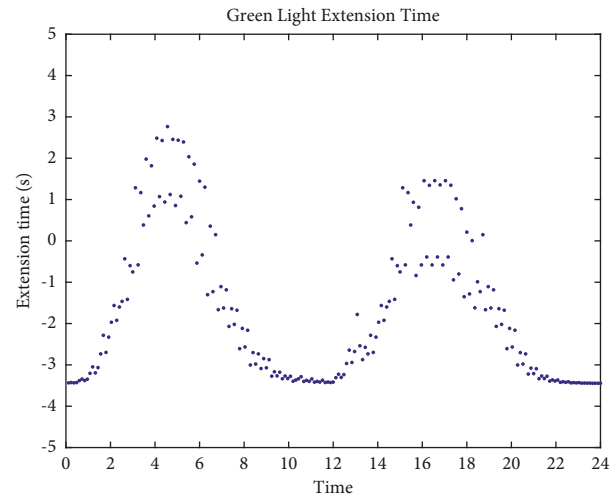


FIGURE 10: Extension time of green lights at different times during a 24-hour day.

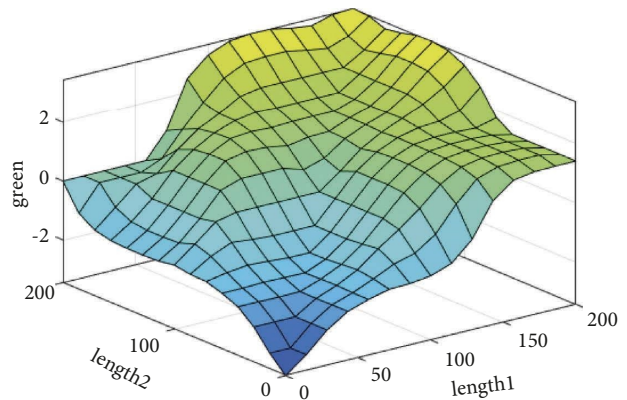


FIGURE 11: Diagram of membership functions for two objectives.

**4.3.1. Implementation of Dynamic Timing.** The Python script is utilized for implementation; E2 detectors are inserted; queue lengths of various phases and lanes are measured using TraCI interface functions; corresponding green light time is searched in the previously calculated data table; and the green light time is inserted into the intersection traffic light using TraCI interface functions. The intersection simulation with the dynamic timing method applied is shown in Figure 13.

**4.3.2. Comparison Analysis of Performance Indicators Before and After Optimization.** The first step involves generating a road network file from netedit, creating nodes, establishing intersections, connecting edges, configuring lane movements, and setting traffic signals for intersections. In the second step, traffic flow files are configured by using randomTrips to generate flows meeting specific criteria. Three different traffic volumes—high, medium, and low—are defined. The third step entails writing a configuration file and running the simulation. Finally, SUMO is used to output values for delay, number of stops, and fuel consumption under various traffic flow conditions.

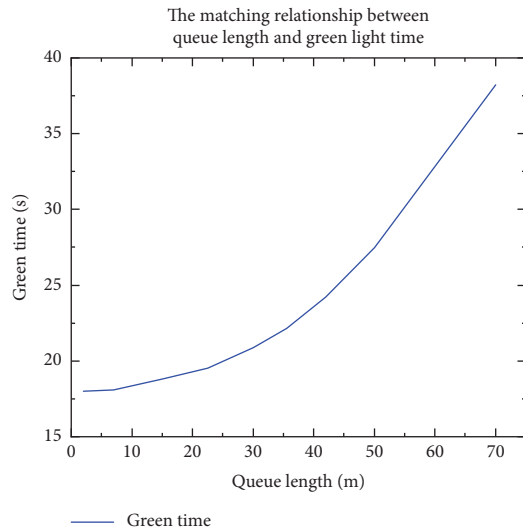


FIGURE 12: Different queue lengths corresponding green light times.

The SUMO software's TraCI interface enables real-time access to delay, congestion, and fuel consumption data. The evaluation metric values of signal timing results optimized by the multiobjective algorithm are compared with those of the initial timing results. Additionally, three scenarios of light, moderate, and heavy traffic flow are set. In this comparison, the indicators after dual-layer optimization are compared with the indicators before optimization under three traffic conditions. The average values of various indicators for both signal timings over the course of a day are compared and presented in Table 4 and Figure 14.

The data above indicates that the algorithm performs better under higher traffic volumes, but overall, it is adaptable to varying traffic conditions.

Additionally, we also compare the evaluation metric values corresponding to the signal timing after the dual-layer optimization with the results of the Webster timing method and the actuated timing method. These three signal timing optimization methods are all implemented in the SUMO simulation software. The Webster timing method and the actuated timing method are executed within SUMO, while our proposed timing optimization method is called externally through the TraCI interface, with all output results generated by SUMO. The specific comparison results are presented in Table 5.

From the table, it can be concluded that our proposed dual-layer optimization method outperforms both the Webster timing method and the actuated timing method in terms of delay, parking rate, and fuel consumption. For example, under heavy traffic flow, the improvement in the delay index is 31.2% compared to the Webster timing method and 18.2% compared to the actuated timing method.

**4.3.3. Comparison of Performance Indicators under Extreme Traffic Conditions and Normal Traffic Conditions.** Since the heavy, medium, and light traffic volume values in the previous section were scaled in proportion to the actual measured traffic, we attempted to analyze the algorithm's

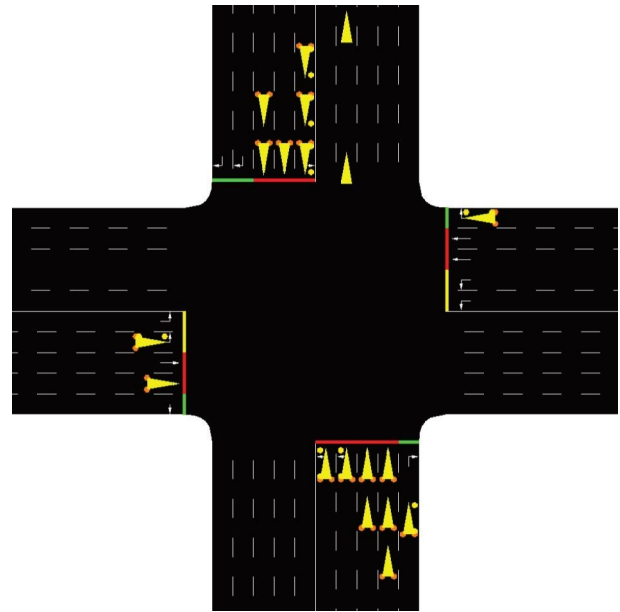


FIGURE 13: Simulated diagram of intersection after signal timing optimization.

effectiveness under more extreme traffic conditions. The intersection conditions remained the same as in the previous simulation setup, with only the traffic volume values changed: the traffic volume in the north-south direction was approximately doubled, and the east-west traffic volume was reduced to about half of the original. At the same time, the inflow and outflow were kept equal; hence,  $I_1 = 1102$  pcu/h,  $I_2 = 337$  pcu/h,  $I_3 = 1416$  pcu/h,  $I_4 = 246$  pcu/h,  $O_1 = 896$  pcu/h,  $O_2 = 361$  pcu/h,  $O_3 = 1410$  pcu/h, and  $O_4 = 434$  pcu/h. Under these traffic conditions, we ran the dual-layer framework signal optimization method and established a signal timing library for different queue lengths. Similar to before, we set up SUMO simulations, monitored queue lengths, invoked corresponding green light durations, and outputted the results for three evaluation indicators: delay, stop rate, and fuel consumption, as shown in Table 6.

As seen from the table, under extreme traffic conditions, due to the excessive flow of traffic in the north-south direction, there may be a certain degree of increased delay, increased parking rates, and increased fuel consumption, though the increase is relatively small. Overall, the traffic condition at the intersection has not been greatly affected. This also indicates that the signal optimization method has basic scalability and can be applied to different types of traffic conditions.

**4.3.4. Comparison of Delay Indicators at Different Times of the Day Before and After Optimization.** The delay values are compared at different traffic volumes during the 24 hours of the day for the initial timing, the basic timing after the first-layer optimization, and the dynamic timing after the two-layer optimization. From Figure 15, it can be observed that the dynamic adjustment of signal timing effectively reduces delays at the intersection. Furthermore, the results of

TABLE 4: Comparison of evaluation indicators at the intersection before and after optimization.

Signal timing conditions	Delay(s)			Parking rate			Fuel consumption (L/h)		
	Light	Medium	Heavy	Light	Medium	Heavy	Light	Medium	Heavy
Before	18	23	31	0.71	0.74	0.80	52	63	78
After	16	19	22	0.67	0.68	0.72	48	55	62
Decrease (%)	11.1	17.4	29.0	5.6	8.1	10.0	7.7	12.7	20.5

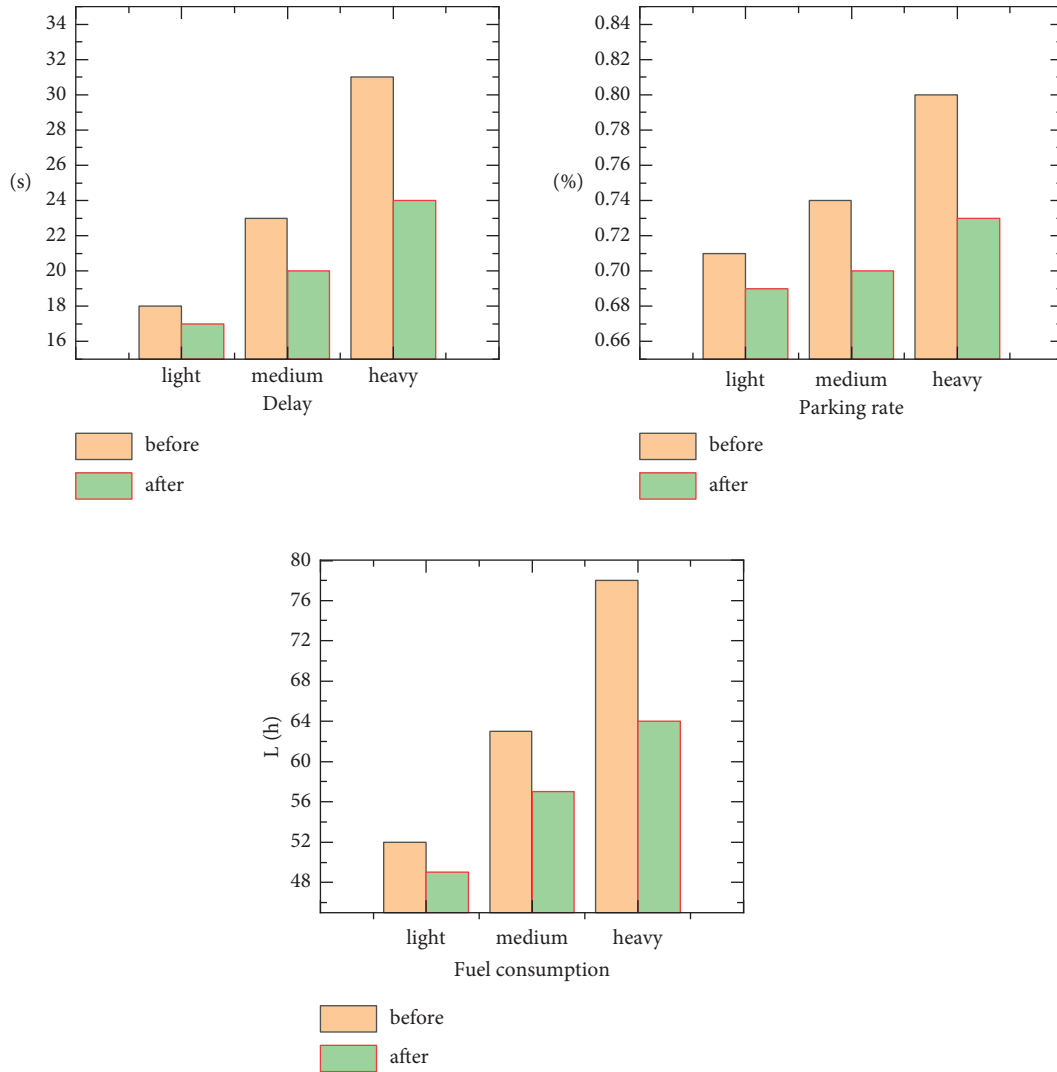


FIGURE 14: Comparison of evaluation indicators.

TABLE 5: Comparison of evaluation indicators for the three optimization methods.

Signal timing conditions	Delay(s)			Parking rate			Fuel consumption (L/h)		
	Light	Medium	Heavy	Light	Medium	Heavy	Light	Medium	Heavy
Webster	18	22	29	0.71	0.73	0.78	52	62	75
Actuated	17	20	26	0.69	0.71	0.74	50	59	67
Dual layer	16	19	22	0.67	0.68	0.72	48	55	62

dynamic adjustment based on the timing optimized by the algorithm outperform those based on the original timing. This is evident in a more significant reduction in delays

during peak hours. Although the optimization effect on delay during nonpeak hours is not as significant, it has a minor impact due to the lower traffic volume.

TABLE 6: Comparison of evaluation indicators for north-south and east-west under two traffic conditions.

Signal timing conditions	Delay(s)		Parking rate		Fuel consumption (L/h)	
	North-south	East-west	North-south	East-west	North-south	East-west
Normal conditions	23	21	0.72	0.72	64	60
Extreme conditions	25	20	0.73	0.72	67	59

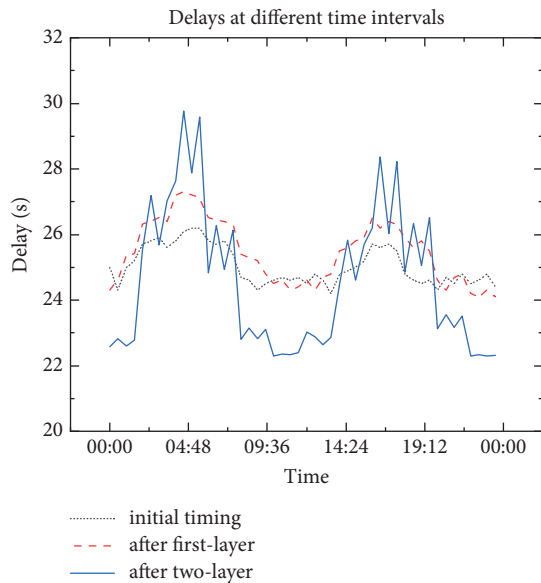


FIGURE 15: Delay at different times of the day for one cycle and two cycles.

The process validated by the above simulation demonstrates that as long as the queue length at intersections can be obtained, the method we proposed can be applied to the timing of traffic lights at intersections. Therefore, in the context of intelligent connected vehicle technologies, our method can also be applied to existing traffic management systems.

## 5. Conclusions

In conclusion, this study has introduced an innovative dual-layer framework for traffic signal optimization, addressing critical urban road traffic management challenges. The first layer used multiobjective optimization, focusing on key performance metrics such as delay, the number of stops, and fuel consumption. The second layer proposes a fuzzy neural network method to learn the correspondence between queue lengths and signal timings. This two-tiered approach enables real-time adjustments, achieving dynamic signal optimization. Applying this framework to a specific road intersection, using real traffic flow data, allows for the dynamic determination of optimal signal timings.

Extensive simulations conducted with the SUMO software validate the efficacy of our approach in significantly reducing delays, with the implemented timing strategy resulting in a noteworthy decrease of 11.1%–29.0% in delay. This dual-layer framework provides valuable theoretical insights for future research initiatives in the domain of signal

control systems. The presented methodology, which combines hybrid multiobjective particle swarm algorithms and fuzzy neural techniques, demonstrates its applicability and effectiveness in optimizing signal timings for enhanced intersection performance.

Furthermore, this paper addresses the growing demand for intelligent transportation solutions. Future research directions should explore multi-intersection coordinated control and large-scale regional collaborative control, contributing to the advancement of intelligent transportation systems with increased practicality and application value.

## Data Availability

The data used to support the findings of this study are included within the article.

## Conflicts of Interest

The authors declare that they have no conflicts of interest.

## Acknowledgments

This research was supported by grants from the National Key Research and Development Program of China (2022YFB2503204) and in part by the National Natural Science Foundation of China (No. 52272420).

## References

- [1] J. H. Mao, Q. W. Tian, and C. P. Lu, "Impact of rapid transit development on urban economic growth: an empirical study of the urban agglomerations in China," *Frontiers in Earth Science*, vol. 10, 2022.
- [2] D. J. Closs and Y. A. Bolumole, "Transportation's role in economic development and regional supply chain hubs," *Transportation Journal*, vol. 54, no. 1, pp. 33–54, 2015.
- [3] C. X. Ma, J. B. Zhou, X. D. Xu, and J. Xu, "Evolution regularity mining and gating control method of urban recurrent traffic congestion: a literature review," *Journal of Advanced Transportation*, vol. 2020, pp. 1–13, 2020.
- [4] T. Q. Zhang, L. S. Sun, L. Y. Yao, and J. Rong, "Impact analysis of land use on traffic congestion using real-time traffic and POI," *Journal of Advanced Transportation*, vol. 2017, pp. 1–8, 2017.
- [5] M. F. Majeed and A. A. Fahad, "Traffic control system techniques: a review," *International Journal of Nonlinear Analysis and Applications*, vol. 13, no. 2, pp. 829–835, 2022.
- [6] I. Seth, K. Guleria, S. N. Panda et al., "A taxonomy and analysis on internet of vehicles: architectures, protocols, and challenges," *Wireless Communications and Mobile Computing*, vol. 2022, pp. 1–26, 2022.
- [7] M. Eom and B. I. Kim, "The traffic signal control problem for intersections: a review," *European Transport Research Review*, vol. 12, no. 1, 2020.

- [8] Q. Q. Guo, L. Li, and X. Jeff Ban, "Urban traffic signal control with connected and automated vehicles: a survey," *Transportation Research Part C: Emerging Technologies*, vol. 101, pp. 313–334, 2019.
- [9] R. H. Yao, X. Y. Wang, H. F. Xu, and L. Lian, "Emission factor calibration and signal timing optimisation for isolated intersections," *IET Intelligent Transport Systems*, vol. 12, no. 2, pp. 158–167, 2018.
- [10] Z. B. Ma, T. C. Cui, W. X. Deng, F. Y. Jiang, and L. G. Zhang, "Adaptive optimization of traffic signal timing via deep reinforcement learning," *Journal of Advanced Transportation*, vol. 2021, pp. 1–14, 2021.
- [11] H. Zhang, S. S. Guo, X. Z. Long, and Y. Y. Hao, "Combined dynamic route guidance and signal timing optimization for urban traffic congestion caused by accidents," *Journal of Advanced Transportation*, vol. 2023, pp. 1–16, 2023.
- [12] Y. Z. Zou, M. Y. Li, J. B. Guo, E. J. Yao, and R. S. Chen, "Vehicle trajectory control and signal timing optimization of isolated intersection under V2X environment," *Journal of Advanced Transportation*, vol. 2023, pp. 1–14, 2023.
- [13] Y. Li, L. J. Yu, S. R. Tao, and K. M. Chen, "Multi-objective optimization of traffic signal timing for oversaturated intersection," *Mathematical Problems in Engineering*, vol. 2013, pp. 1–9, 2013.
- [14] Y. Z. Wang, X. G. Yang, H. L. Liang, and Y. D. Liu, "A review of the self-adaptive traffic signal control system based on future traffic environment," *Journal of Advanced Transportation*, vol. 2018, pp. 1–12, 2018.
- [15] J. Kwak, B. Park, and J. Lee, "Evaluating the impacts of urban corridor traffic signal optimization on vehicle emissions and fuel consumption," *Transportation Planning and Technology*, vol. 35, no. 2, pp. 145–160, 2012.
- [16] X. G. Li, G. Q. Li, S. S. Pang, X. G. Yang, and J. L. Tian, "Signal timing of intersections using integrated optimization of traffic quality, emissions and fuel consumption: a note," *Transportation Research Part D: Transport and Environment*, vol. 9, no. 5, pp. 401–407, 2004.
- [17] J. F. Zhao, W. Li, J. M. Wang, and X. G. Ban, "Dynamic traffic signal timing optimization strategy incorporating various vehicle fuel consumption characteristics," *IEEE Transactions on Vehicular Technology*, vol. 65, no. 6, pp. 3874–3887, 2016.
- [18] R. Qian, Z. Lun, Y. Wenchen, and Z. Meng, "A traffic emission-saving signal timing model for urban isolated intersections," in *13th COTA International Conference of Transportation Professionals (CICTP), Shenzhen, PEOPLES R CHINA, Aug 13-16 2013*, vol. 96, pp. 2404–2413, Procedia Social and Behavioral Sciences, 2013.
- [19] X. W. Han, J. L. Duan, D. Wang, and I. Destech Publicat, "Algorithm of dynamic timing based on multi-objective optimization for urban single intersection traffic light," in *International Conference On Automation, Mechanical And Electrical Engineering (AMEE), Phuket, THAILAND, Jul 26-27 2015*, pp. 807–815, 2015.
- [20] L. Liu and L. Wei, "Research on intersection signal timing based on multi-objective linear combination," *2022 4th International Conference on Artificial Intelligence and Advanced Manufacturing (AIAM)*, 2022.
- [21] X. Li and J. Q. Sun, "Multi-objective optimal predictive control of signals in urban traffic network," *Journal of Intelligent Transportation Systems*, vol. 23, no. 4, pp. 370–388, 2019.
- [22] H. F. Jia, Y. Lin, Q. Y. Luo, Y. X. Li, and H. Z. Miao, "Multi-objective optimization of urban road intersection signal timing based on particle swarm optimization algorithm," *Advances in Mechanical Engineering*, vol. 11, no. 4, p. 168781401984249, 2019.
- [23] A. Sundaram, "Combined heat and power economic emission dispatch using hybrid NSGA II-MOPSO algorithm incorporating an effective constraint handling mechanism," *IEEE Access*, vol. 8, pp. 13748–13768, 2020.
- [24] D. Krajzewicz, "Traffic simulation with SUMO- simulation of urban mobility," in *Fundamentals of Traffic Simulation*, J. Barcelo, Ed., vol. 145, International Series in Operations Research & Management Science, 2010.